USB Proceedings

2014 International Conference on Electrical Machines (ICEM)

Andel`s Hotel Berlin
Berlin, Germany
02 - 05 September, 2014

Sponsored by

The Institute of Electrical and Electronics Engineers (IEEE)
IEEE Industrial Electronics Society (IES)

Co-sponsored by

ETG - Power Engineering Society withing VDI

Performance improvement of a high-speed permanent magnet excited synchronous machine by flux-barrier design

M. Hombitzer, S. Elfgen, D. Franck and K. Hameyer
Institute of Electrical Machines
RWTH Aachen University
marco.hombitzer@iem.rwth-aachen.de

***Abstract*—Due to their high power density and high overall efficiency permanent magnet excited synchronous machines are beneficial to be applied in traction drives of full electric or hybrid-electric vehicles with limited installation space. To improve the performance, additional flux-barriers can be inserted to the rotor of the machine. In this paper, the effects of different flux-barrier positions and sizes are systematically studied. Command variables for the improvement are average torque, torque ripple, total harmonic distortion of the back-emf, iron losses and efficiency.**

***Keywords*—AC-machines, permanent magnet synchronous machines (PMSM), traction motors, energy efficiency, flux-barrier, machine design**

I. Introduction

An increasing traffic volume leads to rising pollution and noise emission. In combination with an increased ecological awareness and political endeavours, research and development focus more and more on alternative vehicles with energy-efficient drive trains and reduced emission. Battery electric vehicles are a promising concept to solve this problem. The main demands for an electric machine as a traction drive in an electric vehicle are high power density and high overall efficiency. Therefore permanent magnet excited synchronous machines with buried magnets (IPMSM) are the most qualified and the mainly applied machines in electric drive trains. To achieve a high power density and a small installation space, the design of machines for high rotational speeds is suitable.

To improve the torque characteristic of IPMSMs in terms of reducing cogging torque and torque ripple, selective flux-barriers can be applied. This can be achieved, for example, by applying additional holes in the rotor [1]-[3], notches in the surface of the rotor [4], [5] or by special shaping of the pockets for the permanent magnets [6], [7]. Furthermore, the average torque can be increased by means of additional flux-barriers [8], [9], due to decreased leakage-flux. In addition, these arrangements influence the shape of the back-electromagnetic-force (back-emf) and can lead to reduced iron losses [2], [7].

Within the scope of the co-operative project *e-generation*, funded by the German Federal Ministry of Education and Research, a traction drive for an electric sports car is developed. Its electrical machine has six poles with V-shaped buried magnets and is designed for a maximum speed of 18.000 rpm. Further reduction of losses and increasing efficiency is aspired to lower the energy consumption and to enhance the operating range of the vehicle. Moreover, a reduction of losses may lead to higher continuous torques and increased overload capabilities.

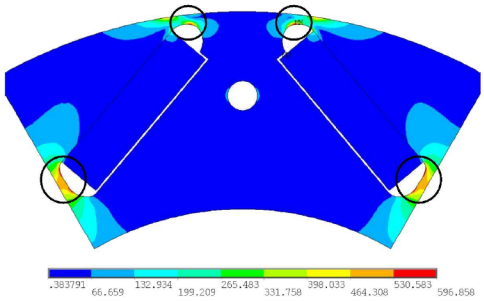

Fig. 1: Von Mises equivalent stress intensity and critical rotor bridges.

This paper presents a study on the influence of circular-shaped flux-barriers on the machine's operating behaviour and presents different rotor configurations to enhance the performance of the machine.

II. Design Approach

To determine the effect of additional flux-barriers in the rotor, various rotor configurations are investigated differing in the number of flux-barriers, their positions and their sizes. Due to the buried positioned permanent magnets, the bridges of the magnet-pockets of the rotor, as shown in Fig. 1, have to be dimensioned for each rotor configuration to minimize leakage flux within the rotor and to ensure mechanical stability over the whole speed range. By means of the von Mises equivalent stress intensity, two stress matrices are simulated for the outer bridges and the bridge at the centre of the V-shaped magnets, varying each bridge's thickness at a time. After eliminating all mechanically unstable variations, a superposition of both matrices delivers the set of minimal bridge thicknesses for the respective rotor geometry. All configurations are designed to endure the required over-speed test speed.

In a first step, two operating points are considered. Characteristic values for speed, torque and mechanical output power can be found in Tab. I. Operating Point 1 (OP1) represents

TABLE I: Characteristic values of the considered operating points.

Parameter	OP1	OP2	Unit
Speed n	6000	6000	min^{-1}
Torque T	150	70	Nm
Mechanical output power P_{mech}	94	44	kW

maximal acceleration of the vehicle, OP2 an operating point of high occurrence. Locked-rotor-tests are conducted to determine the optimal field-weakening angles and the proportion of synchronous- and reluctance torque on the overall torque [10]. Operating point simulations are performed by using the optimal field-weakening angle to set the maximum torque with minimal current. In order to achieve comparability in terms of thermal stress of the different designs, a constant slot-side loading is ensured.

The different rotor configurations are compared regarding torque, induced voltage and efficiency. Torque is analysed by its average value, torque ripple and the ratio of synchronous torque and reluctance torque. Concerning the induced voltage its total harmonic distortion is analysed. For calculating the machine's efficiency, copper losses, iron losses and mechanical losses, caused by air friction and bearing friction, are regarded. Iron losses are calculated with the *IEM-5-Parameter-Formula* assessing stator and rotor iron losses, separated into hysteresis losses, eddy-current losses, excess losses and non-linear losses [11].

Based on the described method, a selection of promising rotor configurations is analysed in detail regarding the whole operating range of the electrical machine up to 18.000 rpm.

III. Symmetrical Flux-Barrier Locations

To study the general impact of flux-barriers on the machine's operating behaviour, flux-barriers located symmetrical to the rotor poles are applied. First, single barriers are studied, positioned in the magnetic d-axis or the magnetic q-axis of the rotor. A third symmetrical variation is done by applying two flux-barriers symmetrical to the magnetic d-axis in tangential direction referring to the outer radius of the rotor.

A. Variation in magnetic d-axis

Fig. 2 demonstrates the evaluated positions with exemplary diameters of the flux-barrier variation in the magnetic d-axis. The flux-barriers can be described by the angle φ_b related to the segment of one pole pair, the distance from the origin R_m and the hole diameter D_b. The investigation of four hole diameters and five selected positions result in twenty different rotor designs. The lowest barrier position ($R_m = 33.25\,\text{mm}$) is placed directly under the central bridge. Above the permanent magnets, positions are distributed evenly from $R_m = 14.45\,\text{mm}$ to $R_m = 47.25\,\text{mm}$.

Locked rotor tests reveal a correlation between the flux-barrier diameter and the resulting torque, analysed in operating point one. Rising hole diameters lead to a slightly decreasing reluctance torque. Barriers positioned above the centre bridge do not influence the synchronous torque. The total torque decreases up to 2% with rising hole diameters. Applying a

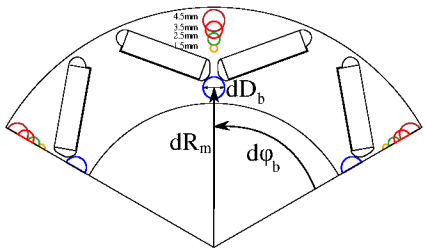

Fig. 2: Exemplary diameters and positions of the flux-barrier variation in magnetic d-axis.

flux-barrier with the smallest considered hole diameter beneath the centre bridge leads to an increase of the average torque up to 2%. The reason is an increasing synchronous torque because of a lower leakage-flux at the centre bridge. For larger hole diameters the bridge thickness has to be increased to ensure mechanical stability. This leads to a reduced magnet width on condition that the opening angle of the V-shaped pole and the pole pitch factor remain constant. As shown in Fig. 3, rising hole diameters lead to higher relative torque ripples, especially for the barrier position beneath the centre bridge.

Corresponding to torque ripple, the THD of the back-emf increases along with a rising flux-barrier diameter. In contrast, the maximum value shows a different behaviour concerning positions above and below the centre bridge. In both operating points a rising maximum value can be achieved at the lower barrier position. Flux-barriers above the centre bridge reduce the maximum value of the back-emf. As a result the total harmonic distortion of the back-emf is affected negatively by applying flux-barriers in the magnetic d-axis.

The influence of the different flux-barrier positions and diameters on the stator and rotor iron losses in operating point one is shown in Fig. 4. Fig. 4a indicates the positive impact of flux-barriers on stator iron losses. The biggest barrier next to the rotor outside radius reduces the stator iron losses up to 6 %. While all stator loss components are decreased, the reduction is primarily based on lower non-linear losses. On the other hand slightly higher rotor iron losses arise with an increased diameter of the flux-barriers, Fig. 4b. It can be found that the

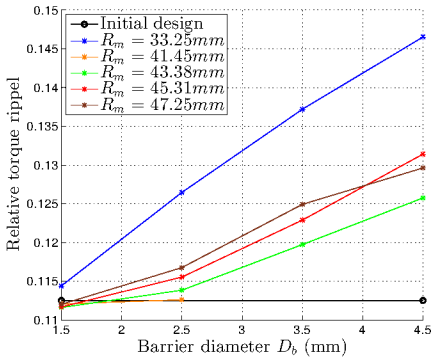

Fig. 3: Influence of flux-barrier diameter in d-axis on the torque ripple.

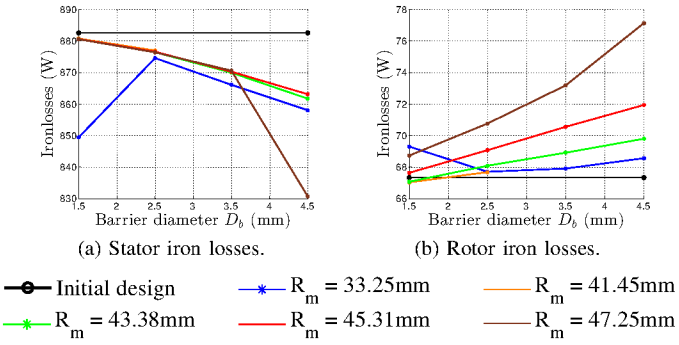

(a) Stator iron losses. (b) Rotor iron losses.

Fig. 4: Influence of flux-barrier diameter in d-axis on iron losses.

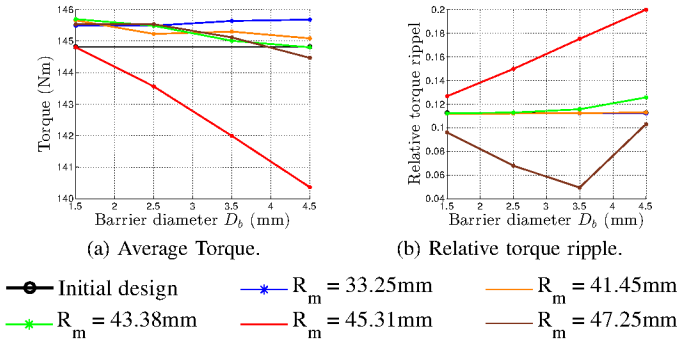

(a) Average Torque. (b) Relative torque ripple.

Fig. 6: Influence of flux-barrier diameter in q-axis on the torque.

size of the flux-barrier as well as its local position strongly influence the additional eddy current losses.

In consequence, a flux-barrier placed in the magnetic d-axis does not improve the torque performance as well as the back-emf. However, the total iron losses can be reduced by applying additional flux-barriers.

B. *Variation in magnetic q-axis*

Flux-barriers in the magnetic q-axis, Fig. 5, are analysed starting with the locked rotor test. Three different types of characteristic effects can be seen. The three positions closest to the center ($R_m = 33.25\,\mathrm{mm}, R_m = 41.45\,\mathrm{mm}$ and $R_m = 43.38\,\mathrm{mm}$) do not affect the torque. Whereas a flux-barrier placed in the q-axis at the nearest position between two magnets ($R_m = 45.31\,\mathrm{mm}$) is causing a significant shift from the reluctance torque towards the synchronous torque. The sum of both torque components is decreasing. In the following, this barrier position will be referred to as position four. The third characteristic influence on the machine's torque comes from position five close to the rotor outside radius ($R_m = 47.25mm$), also reducing the reluctance but not affecting the synchronous torque.

The influence of the flux-barriers' diameter on the average torque and the torque ripple in the selected operating point is presented in Fig. 6. As seen in the locked rotor test, the three barrier positions close to the centre have nearly no influence on the torque performance at all. The reason is found in the low local flux densities, where barriers have no significant flux shaping effect.

When concerning the average torque, the decreasing characteristic of barrier position four is remarkable. At this position, larger flux-barriers lead to significantly higher local flux densities between the barrier and the pocket of the permanent magnets. Consequently the reduced average torque is reflected by a higher relative torque ripple increasing linearly with the hole diameter, which can be seen for both operating points. The second characteristic regarding the relative torque ripple is placed at position five, closest to the rotor outside radius. A local minimum is found at a hole diameter of 3.5 mm in operating point one. In contrary the relative torque ripple in the second operating point increases due to the changed flux distribution. The smallest barrier diameter at this position is chosen for further investigations.

Fig. 7 shows the comparison of the torque characteristics of the initial design with the lowest and highest resulting torque ripple caused by added flux-barriers in the magnetic q-axis in operating point one. It leads to the conclusion that a rising flux-barrier diameter between the magnets of two poles lowers the minimum value of the torque oscillation, keeping the maximum on a constant value. In contrast, the upper barrier position lowers both the maximum and minimum value, resulting in lower relative torque ripple and a slightly higher average torque. The impact of the flux-barriers on torque harmonics is depicted in Fig. 7b. The amplitude of

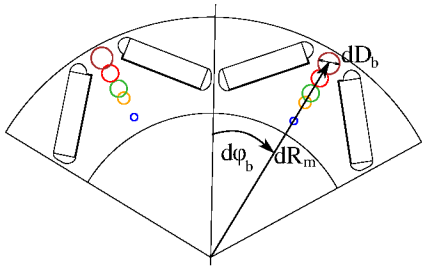

Fig. 5: Exemplary diameters and positions of the flux-barrier variation in magnetic q-axis.

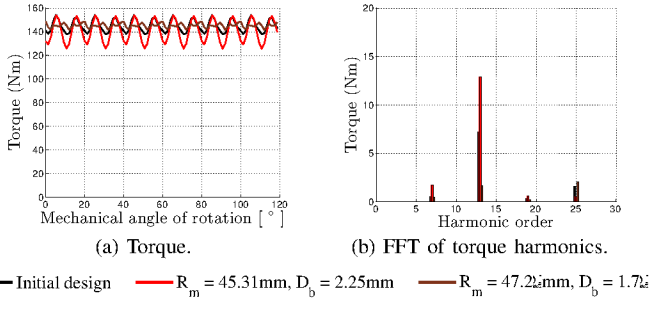

(a) Torque. (b) FFT of torque harmonics.

Fig. 7: Influence of flux-barrier diameter in q-axis on the torque

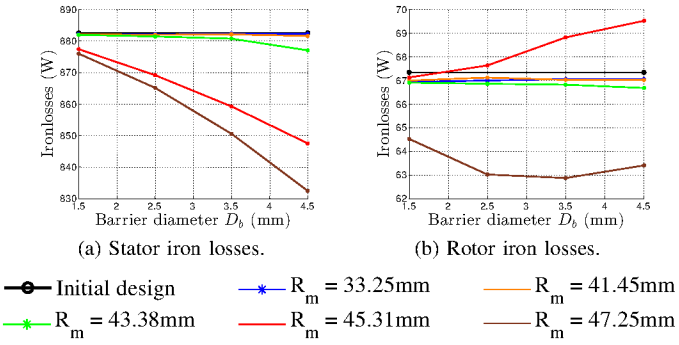

(a) Stator iron losses. (b) Rotor iron losses.

Fig. 8: Influence of flux-barrier diameter in q-axis on iron losses.

the fundamental cogging torque harmonic, identified as 12^{th} harmonic and its sub-harmonics are notably excited in the case of additional flux-barriers being applied.

In operating point one the THD of the back-emf increases with the diameter for each barrier position. The positions four and five ($R_m = 45.31\,\mathrm{mm}$, $R_m = 47.25\,\mathrm{mm}$) discussed before differ in their effect on the maximum value of the back-emf. The maximum value of the back-emf is increased at barrier position 4 and decreased at barrier position five. This opposing influence indicates the sensitivity of the discussed positions underlining the need of a closer optimization process. In operating point two, barrier position five reveals an improvement of the THD of the back-emf for barrier diameters up to 3.5 mm, confirming the choice of small diameters for a further analysis.

Both stator and rotor iron losses are influenced by the barrier positions in the same way as seen at previous parameters, Fig. 8. The first three positions do not affect the machine's operating performance, while positions four and five have a high impact. Stator iron losses are reduced by up to 6 % corresponding to the barrier diameter. Again, the reduction of non-linear losses is the main reason. In contrary to all variations in the magnetic d-axis a small improvement of rotor losses is achieved by flux-barriers applied in position five.

In consequence, only two positions of the studied configurations of flux-barriers in the magnetic q-axis show a significant influence on the machine's performance. Flux-barriers applied at position four result in a negative impact on all analysed parameters except iron losses. Whereas position five shows improvements especially for barriers with small diameters.

C. Variation in tagential direction

The third symmetrical variation is performed by applying flux-barriers in tangential direction according to the rotor outside radius. In general, two different starting areas are possible: above and below the permanent magnets. Flux-barriers positioned below the magnets turned out to be ineffective or even detrimental in their effects on the machine's performance. Therefore only barriers close to the rotor outside radius will be discussed. Fig. 9 presents all barrier positions and exemplary the two examined diameters. In contrast to the symmetrical alignment in d- and q-axis, a total number of two holes per

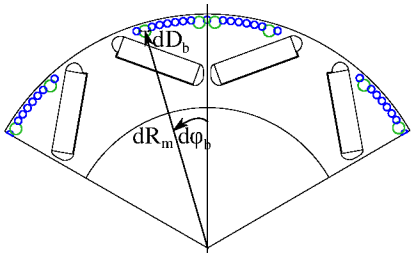

Fig. 9: Exemplary diameters and positions of the flux-barrier variation in tangential direction.

pole are applied, positioned symmetrical to the magnetic d-axis.

The barriers are studied in an interval of $\varphi_b = 2\,^\circ$. With rising position angle, the synchronous torque increases while the reduction of the reluctance torque converges at $12\,^\circ$ during the locked rotor test. Fig. 10 shows the resulting torque characteristic in operating point one. The average torque does not show significant changes in both operating points. However a strong dependency between the flux-barrier angle and the relative torque ripple is determined for both operating points. Fig. 10b demonstrates the changing influence of the flux-barriers on the torque ripple. A minimum can be found at $\varphi_b = 10\,^\circ$ whereas a maximum can be seen at a position of $\varphi_b = 15\,^\circ$.

The found periodicity accords to half of the slot pitch angle. Its characteristic can also be seen for the THD and maximum value of the back-emf with local extrema at the mentioned angles. As previously determined for variations in magnetic q-axis, smaller hole diameters achieve a more advantageous behaviour.

Stator and rotor iron losses in operating point one are depicted in Fig. 11. Flux-barriers show a positive impact on the iron losses in both operating points, increasing with the hole diameter and depending on the position. The local minimum seen at the back-emf and torque complies with the characteristic of the stator iron losses. Flux-barriers indicate no further correlation between the position angle and rotor iron losses.

Taking all symmetrical variations into account, flux-barriers

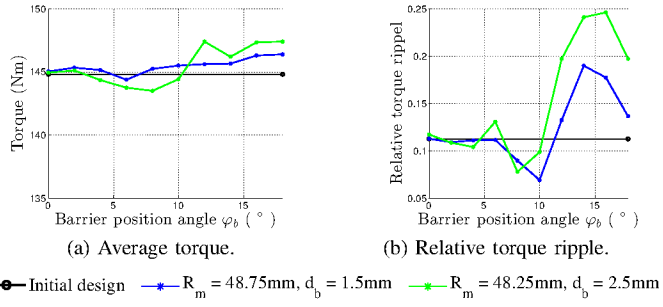

(a) Average torque. (b) Relative torque ripple.

Fig. 10: Influence of flux-barrier variation in tangential direction on the torque.

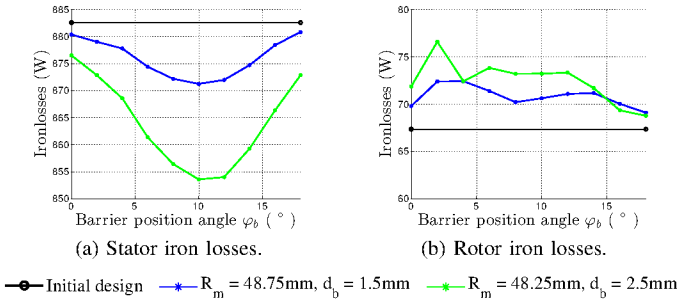

(a) Stator iron losses. (b) Rotor iron losses.

Fig. 11: Influence of flux-barrier variation in tangential direction on iron losses.

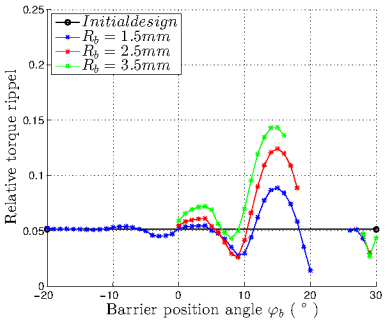

Fig. 13: Influence of asymmetrical flux-barrier variation in tangential direction on torque ripple.

in the magnetic d-axis are not further investigated. The favourable barrier position in the magnetic q-axis below the rotor outside radius is similar to the last analysed tangential flux-barrier configuration. Consequently, radial positioning of the barriers is studied further.

IV. Asymmetrical Flux-Barrier Locations

When used in a traction drive of an electric vehicle, the electrical machine has a preferred rotational direction. To take advantage of this, asymmetrical flux-barrier positions relative to the rotor poles are investigated. Fig. 12 illustrates configurations with single flux-barriers and configurations with two barriers of a constant distance.

A. Single barriers

Locked rotor tests with single asymmetrical flux-barriers show no influence of the synchronous torque while the reluctance torque is slightly reduced, whereas symmetrical configurations result into a shift between the torque components. In operating point one, a small increase of the average torque value is achieved, however, revealing an indifferent characteristic regarding the torque ripple. Fig. 13 demonstrates the correlation between the flux-barrier position angle and the torque ripple for different diameters of the holes, forming a periodicity similar to the symmetrical variations. The proposed period length of half the slot pitch angle is verified with local minima at 10 ° and 20 °. Furthermore, the torque ripple characteristic approves the pole part facing the rotating direction as determinant area in terms of torque performance, also gaining

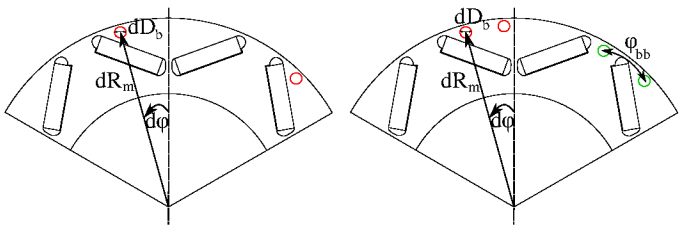

(a) Single asymmetrical barrier. (b) Asymmetrical barriers with constant distance.

Fig. 12: Exemplary rotor configurations with asymmetrical flux-barriers.

impact by rising position angle and hole diameter. Analysing the torque harmonics demonstrates a reduced cogging torque main wave for the 12^{th} and 24^{th} harmonics.

Moreover, the THD and maximum values of the back-emf follow a shape similar to the symmetrical designs however steadily increasing with hole diameter and position angle. Both THD and maximum value show an oscillating characteristic. Stator iron losses decrease to a nearly constant value in contrast to the curve shape for symmetrical variations, which is only reflected in the eddy-current losses.

B. Barrier combinations with a constant distance

Furthermore, the effect of a constant distance between two barriers at different positions within the rotor is analysed. The selected dimensions are based on the symmetrical variation in radial direction. As selection criteria the reviewed parameters are used, namely torque ripple and average torque, secondly THD and maximum value of the back-emf and thirdly rotor and stator iron losses. Local optima are verified at position angles of 10 ° and 20 ° equaling a distance of 20 ° and 40 °. In addition, a distance of 36 ° is tested which showed a deterioration of performance before.

The resulting relative torque ripple, the THD of the back-emf, a torque curve and its harmonic content are shown in Fig. 14. Comparing the two resulting torque ripple curves in Fig. 14a and Fig. 13 reveals no difference between asymmetrical single and double barriers. This result sustaines the conclusion drawn before. The pole part facing the rotating direction is the determinant area in terms of torque performance. The comparison of the torque resulting from the initial rotor design with the one resulting from a double barrier position with minimal torque ripple is presented in Fig. 14c. With a Fourier transformation a strong decrease of the cogging torque harmonic can be seen in Fig. 14d. Variations of flux-barriers with a distance of 40 ° only result in an improved torque ripple for the symmetrical design. The rotor design with a distance of 36 ° leads to the expected negative performance.

However, the THD of the back-emf is affected differently by asymmetrical variations. Those cause an increase of higher harmonics in the back-emf, while certain symmetrical designs show an improved THD. The iron losses are influenced in the same way as seen before in terms of increasing rotor iron losses and decreasing stator iron losses.

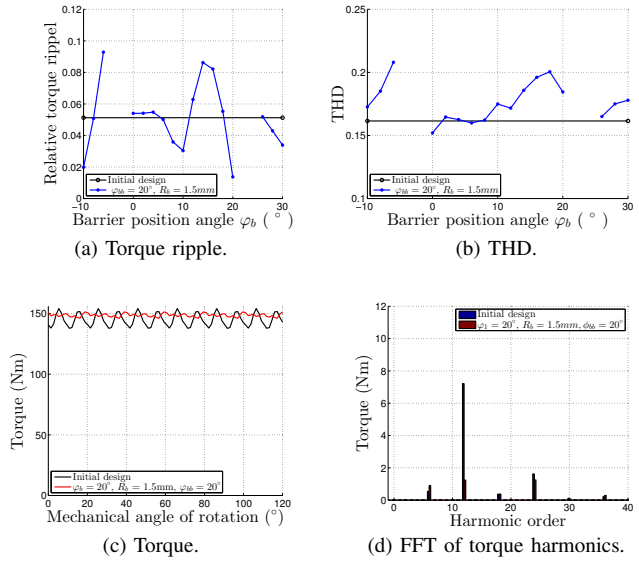

(a) Torque ripple. (b) THD.

(c) Torque. (d) FFT of torque harmonics.

Fig. 14: Influence of asymmetrical flux-barrier variation with a constant distance in tangential direction on torque performance.

V. Performance in Characteristic Diagrams

Promising rotor configurations, selected from the previous investigations, are simulated in characteristic diagrams. Thereby transferability of the results from the previous two operating points to the whole operating area including field-weakening range is reviewed. Moreover, a complete simulation is indispensable to finally assess the chosen designs. In addition to the designs described, symmetrical combinations of flux-barriers are analysed. Therefore, rotor configurations improving the machine's performance at the investigated operating points are combined in order to verify the possibility of superposing effects. As a result, combinations of advantageous flux-barriers do not lead to a further improvement. Instead, an opposite tendency is reviewed at several constellations. Furthermore, the high sensitivity regarding the exact positioning in the magnetic q-axis can be confirmed.

In the following an exemplary flux-barrier design with symmetrical flux-barriers applied to the magnetic q-axis of the rotor is discussed in characteristic diagrams and is compared to the initial rotor design. The cross section of one pole pair of the rotor is depicted in Fig. 15. As expected, due to a decrease of iron losses by up to 15 % across the characteristic map, the area of maximum efficiency is extended towards higher driving speeds, Fig. 16a and Fig. 16d.

The torque ripples, Fig. 16b and Fig. 16e, are depicted as relative torque ripple in the second quadrant of the d-q-current density plane. It is apparent, that flux-barriers reduce torque ripple at current densities around $J_d > 5\ \frac{A}{m^2}$ considerably. The influence on the THD of the back-emf is presented in Fig. 16c and Fig. 16f.

The transferability of the results from the two operating points can be confirmed. Nevertheless, the selection of an optimal rotor design is defined by the individual application.

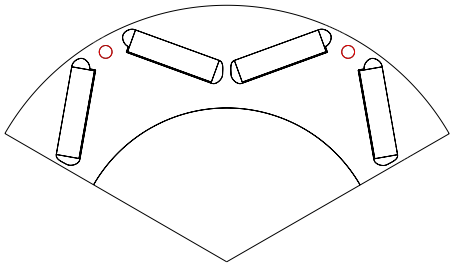

Fig. 15: Exemplary rotor design discussed in characteristic diagrams.

A duty cycle for example has to clarify the most beneficial variation.

VI. Conclusion

This paper focuses on the effect of circular-shaped flux-barriers in the rotor of a permanent magnet excited synchronous machine with V-shaped rotor poles as a traction drive of an electric vehicle. The performance improvement is studied in terms of average torque, torque ripple, total harmonic distortion of the back-emf, stator iron losses, rotor iron losses and efficiency. Rotor configurations with flux-barriers symmetrical to the magnetic poles are studied as well as asymmetric configurations. All rotor configurations consider mechanical stress calculations to assure a sufficient mechanical strength. After considering two exemplary operating points, promising configurations are investigated in detail regarding the whole operating range in characteristic diagrams. Different rotor configurations with additional flux-barriers are presented to reduce torque harmonics and iron losses. Therefore the regions of high efficiency in the efficiency map can be enhanced in comparison to the initial rotor design. Furthermore, operating points at high speeds and high torques can be operated for longer times without overheating due to reduced losses.

A prototype of the initial design is built up to validate the design goals of the machine. For the future it is conceivable to build up some prototypes of the presented rotor configurations to verify the simulation results in practice.

VII. Acknowledgement

This paper was developed in the context of the co-operative project *e-generation* sponsored by the German Federal Ministry of Education and Research, reference number 13N11867.

References

[1] A. Kioumarsi, M. Moallem, and B. Fahimi, *Mitigation of Torque Ripple in Interior Permanent Magnet Motors by Optimal Shape Design*, IEEE Transactions on Magnetics, vol. 42, no. 11, pp. 3706-3711, Nov. 2006.

[2] J. Jang, H. Kim, J. Song, Y. Lee, and B. Kim, *Design of flux barriers in a rotor of an interior PM synchronous motor for reducing harmonics losses*, in 2010 14th Biennial IEEE Conference on Electromagnetic Field Computation (CEFC), 2010, p. 1.

[3] A. Kiyoumarsi and M. Moallem, *Optimal Shape Design of Interior Permanent-Magnet Synchronous Motor*, in 2005 IEEE International Conference on Electric Machines and Drives, 2005, pp. 642-648.

[4] S. Huang, J. Liu, J. Gao, and L. Xiao, *Optimal design of the rotor structure for interior permanent magnet synchronous motor*, in 2011 International Conference on Power Engineering, Energy and Electrical Drives (POWERENG), 2011, pp. 1-5.

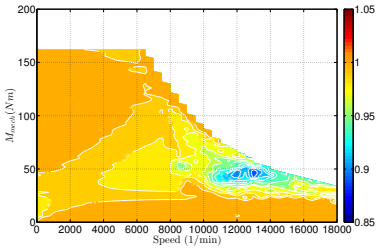

(a) Ratio of total losses of initial and modified design.

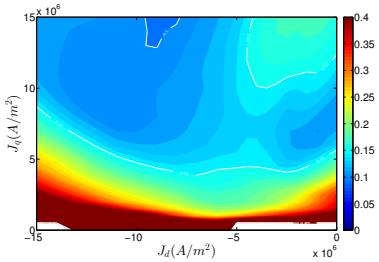

(b) Relative torque ripple of the initial rotor design.

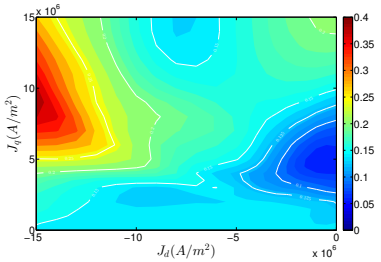

(c) THD of the back-emf of the irotor design.

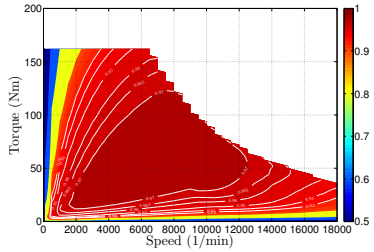

(d) Efficiency of modified rotor design.

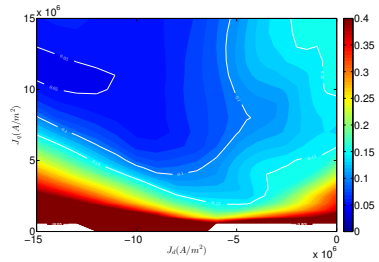

(e) Relative torque ripple of modified rotor design

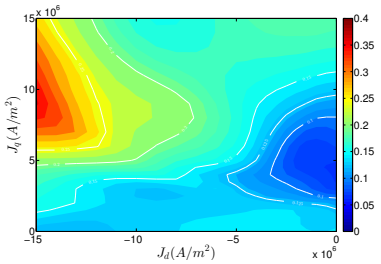

(f) THD of back-emf of the modified rotor design.

Fig. 16: Comparison between the former and modified rotor design, with symmetrical flux-barriers at 30 °.

[5] G.-H. Kang, Y.-D. Son, G.-T. Kim, and J. Hur, *A Novel Cogging Torque Reduction Method for Interior-Type Permanent-Magnet Motor*, IEEE Transactions on Industry Applications, vol. 45, no. 1, pp. 161-167, Jan. 2009.

[6] Y. Kano, T. Terahai, T. Kosaka, N. Matsui, and T. Nakanishi, *A new flux-barrier design of torque ripple reduction in saliency-based sensorless drive IPM motors for general industrial applications*, in IEEE Energy Conversion Congress and Exposition (ECCE), 2009, pp. 1939-1945.

[7] K. Yamazaki, M. Kumagai, T. Ikemi, and S. Ohki, *A Novel Rotor Design of Interior Permanent-Magnet Synchronous Motors to Cope with Both Maximum Torque and Iron-Loss Reduction*, IEEE Transactions on Industry Applications, vol. 49, no. 6, pp. 2478-2486, Nov. 2013.

[8] Y. Park, J.-H. Cho, S.-G. Song, D.-H. Chung, J. So, and D. Kim, *Study on reducing cogging torque of Interior PM Motor for electric vehicle*, in 2012 IEEE Vehicle Power and Propulsion Conference (VPPC), 2012, pp. 171-175.

[9] M. H. Zadeh, A. Kiyoumarsi, and H. Khosravi, *Average torque optimization in interior permanent magnet synchronous motors*, in 18th International Conference on Electrical Machines (ICEM), 2008, pp. 1-4.

[10] M. Hafner, T. Finken, M. Felden, and K. Hameyer, *Automated Virtual Prototyping of Permanent Magnet Synchronous Machines for HEVs*, IEEE Transactions on Magnetics, vol. 47, no. 5, pp. 1018-1021, May 2011.

[11] D. Eggers, S. Steentjes, and K. Hameyer, *Advanced Iron-Loss Estimation for Nonlinear Material Behavior*, IEEE Transactions on Magnetics, vol. 48, no. 11, pp. 3021-3024, Nov. 2012.

VIII. Biographies

Marco Hombitzer received the diploma in electrical engineering from the Faculty of Electrical Engineering and Information Technology, RWTH Aachen University, Aachen, Germany, in 2010. Since 2010, he has been a researcher at the Institute of Electrical Machines. His research fields include the simulation, the design and performance improvement of electrical machines.

Silas Elfgen received the M.Sc. degree in electrical engineering from RWTH Aachen University, Aachen, Germany, in November 2013. After that he has been working as a research associate at the Institute of Electrical Machines. His research interests include soft magnetic materials, simulation and performance improvement of the electrical machines.

David Franck received the Dipl.-ing. degree in electrical engineering from RWTH Aachen University, Aachen, Germany, in March 2008. After that he became of staff (research associate) at the Institute of Electrical Machines. Since 2011 he has been working as chief engineer of the Institute of Electrical Machines. His main field of research is the acoustic behaviour of the electrical machines.

Dr. Kay Hameyer received his M.Sc. degree in electrical engineering from the University of Hannover and his Ph.D. degree from the Berlin University of Technology, Germany. After his university studies he worked with the Robert Bosch GmbH in Stuttgart, Germany as a Design Engineer for permanent magnet servo motors and vehicle board net components. Until 2004 Dr. Hameyer was a full Professor for Numerical Field Computations and Electrical Machines with the KU Leuven in Belgium. Since 2004, he is full professor and the director of the Institute of Electrical Machines (IEM) at RWTH Aachen University in Germany. 2006 he was vice dean of the faculty and from 2007 to 2009 he was the dean of the faculty of Electrical Engineering and Information Technology of RWTH Aachen University. His research interests are numerical field computation and optimisation, the design and controls of electrical machines, in particular permanent magnet excited machines, induction machines and the design employing the methodology of virtual reality. Since several years Dr. Hameyers work is concerned with the magnetic levitation for drive systems, magnetically excited audible noise in electrical machines and the characterisation of ferro-magnetic materials. Dr. Hameyer is author of more than 250 journal publications, more than 500 international conference publications and author of 4 books. Dr. Hameyer is a member of VDE, IEEE senior member, fellow of the IET.